

Evidence for gap anisotropy in CaC_6 from directional point-contact spectroscopy

R.S. Gonnelli,¹ D. Daghero,¹ D. Delaude,¹ M. Tortello,¹ G.A. Ummarino,¹

V.A. Stepanov,² J.S. Kim,³ R.K. Kremer,³ A. Sanna,⁴ G. Profeta,⁵ and S. Massidda⁶

¹*Dipartimento di Fisica and CNISM, Politecnico di Torino, 10129 Torino, Italy*

²*P.N. Lebedev Physical Institute, Russian Academy of Sciences, 119991 Moscow, Russia*

³*Max-Planck-Institut für Festkörperforschung, D-70569 Stuttgart, Germany*

⁴*Institut für Theoretische Physik, Freie Universität Berlin, Arnimallee 14, D-14195 Berlin, Germany*

⁵*CNISM - Dipartimento di Fisica, Università degli studi dell'Aquila, Italy*

⁶*SLACS-INFN/CNR and Dipartimento di Fisica, Università degli Studi di Cagliari, Italy*

We present the first results of directional point-contact spectroscopy in high quality CaC_6 samples both along the ab plane and in the c -axis direction. The superconducting order parameter $\Delta(0)$, obtained by fitting the Andreev-reflection (AR) conductance curves at temperatures down to 400 mK with the single-band 3D Blonder-Tinkham-Klapwijk model, presents two different distributions in the two directions of the main current injection, peaked at 1.35 and 1.71 meV, respectively. By ab-initio calculations of the AR conductance spectra, we show that the experimental results are in good agreement with the recent predictions of gap anisotropy in CaC_6 .

PACS numbers: 74.50.+r, 74.45.+c, 74.70.Ad

The discovery of a relatively “high- T_c ” superconductivity in graphite intercalated with Ca [1, 2], Yb [1] and, very recently, Sr [3, 4] has strongly revived the interest in the Graphite Intercalated Compounds (GICs) and their physics. The Ca-intercalated graphite, CaC_6 , with its “record” T_c of about 11.5 K, in particular, has been the subject of various theoretical and experimental investigations in the past two years (for a short review of the initial results see [5]). One of the most important questions, however, is still not clear: what is the magnitude and anisotropy of its superconducting gap? The first experiments (STM, penetration depth, specific heat) on CaC_6 have evidenced a single, apparently isotropic, s-wave gap with a ratio $2\Delta/k_B T_c$ of the order of the BCS value [6, 7, 8]. Recent tunnel spectroscopy results, on the other hand, claimed the presence of an isotropic gap with a magnitude more than 40% higher than that reported earlier [9]. The spread of gap values measured up to now range between 1.6 meV [6] and 2.3 meV [9]. The important point is that all these experiments have either probed a bulk property [8] or a directional one along the c -axis direction [6, 7, 9]. As pointed out in Ref.6, the presence of anisotropic or two-gap superconductivity in CaC_6 cannot be ruled out until tunneling or point-contact measurements are performed also along the ab direction. On the other hand, recent first-principles density functional calculations of the superconducting properties of CaC_6 have supported the presence of a moderately anisotropic gap which varies between 1.1 and 2.3 meV, depending on the \mathbf{k} -point and the π or interlayer (IL) sheet of the Fermi surface (FS) involved [10]. Such an anisotropy can be revealed by directional spectroscopy measurements performed along both c and ab direction.

In this paper we present the results of point-contact Andreev-reflection (PCAR) spectroscopy performed on high-quality bulk samples of CaC_6 [8]. By using a spe-

cial technique to realize the contacts, that proved very successful and effective in the case of MgB_2 [11, 12], we were able to perform directional PCAR spectroscopy at very low temperature both along the ab plane and the c -axis direction. Two different gap distributions in the two directions can reproducibly be extracted from the experimental data. When compared to the results of new first-principles calculations these findings unequivocally prove the anisotropy of the superconducting gap in CaC_6 .

The high-quality CaC_6 bulk samples used for our measurements were synthesized by reacting highly oriented pyrolytic graphite (with a spread of the c axis orientation $\leq 0.4^\circ$) for several weeks at 350°C with a molten alloy of Li and Ca [8]. The resulting CaC_6 samples have a shiny golden surface. They are very sensitive to air and moisture which rapidly damage the sample surfaces. X-ray analysis has shown mainly the CaC_6 reflections with a small ($< 5\%$) contribution from impurity phases. Further details on the characterization of the samples may be found in Ref. 8. All samples used for PCAR spectroscopy (size $\approx 1 \times 1 \times 0.2 \text{ mm}^3$) were selected to have a very sharp superconducting transition ($\Delta T_c(10\% - 90\%) = 0.1 \text{ K}$) with the onset at $T_c = 11.4 \text{ K}$.

The point contacts were made by using a non-conventional technique we called “soft” PCAR spectroscopy [11, 12]. Instead of using the standard metallic tip, a very small ($\varnothing \simeq 50 \mu\text{m}$) drop of Ag conductive paint, put on the etched or freshly cleaved surfaces of the sample is used as a counterelectrode. Such contacts are particularly stable both in time and towards temperature variations and they allow to inject the current mainly perpendicular to the contact plane. A fine tuning of the junction characteristics at low temperature can be done by applying short voltage or current pulses. Further details on the technique can be found in Refs. 11, 13. Due to the mentioned high sensitivity of CaC_6 samples’

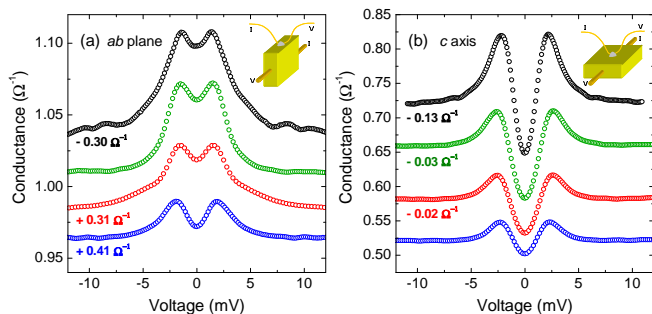


FIG. 1: (Color online) (a) Raw point-contact conductance curves of various ab -plane contacts at 4.2 K. For clarity the curves are vertically shifted of the amount shown close to each curve. (b) The same as in (a) but for various contacts with current injection mainly along the c axis. In each panel a sketch of the contact geometry is also shown.

surface to air, the room-temperature preparation of the contact was done inside a sealed glove bag filled with pure He gas or in a glove box with Ar atmosphere. After the contact was made the junction was very rapidly transferred to the cryostat in a sealed container. Contacts were made either on the flat ab -plane surface or on the narrow lateral side of the samples. Referring to the main direction of current injection, we call them c -axis and ab -plane contacts, respectively (see insets of Fig. 1).

The conductance curves, dI/dV vs. V , were obtained by numerical differentiation of the measured $I-V$ curves and subsequently normalized by dividing them by the normal-state conductance measured at $T \geq T_c$. For this reason, in all the contacts, we therefore carefully studied the temperature dependence of the conductance in order to determine the critical temperature of the junction, i.e. the ‘Andreev critical temperature’, T_c^A . In an overall of 35 different contacts, T_c^A was found to be 11.3 ± 0.1 K, in best agreement with the bulk T_c ’s of the samples and in contrast with a previous report [6]. This fact proves the high quality of samples and surfaces in the contact region. For simplicity, we will therefore refer to the critical temperatures of the contacts as T_c in the following.

Fig. 1 shows several raw conductance curves as function of bias voltage measured both in ab -plane contacts (a) and in c -axis ones (b) at 4.2 K. The curves show clear Andreev-reflection (AR) features, an almost flat conductance (at $V > 8 - 10$ meV) and no dips that usually are a sign of the failure in reaching the conditions for pure ballistic conduction in the contact [14, 15]. The normal resistance R_N of all the good contacts is between 0.75 and 6.4 Ω . By knowing the mean free paths and the residual resistivities of CaC_6 along the ab plane and in the c -axis direction, i.e. $\ell_{ab} = 74$ nm, $\ell_c = 4.7$ nm, $\rho_{0,ab} = 0.8 \mu\Omega\text{-cm}$ and $\rho_{0,c} = 24 \mu\Omega\text{-cm}$ [16, 17] we can apply the Sharvin formula for the contact resistance in the ballistic regime in order to determine the contact radius $a = (4\rho_0\ell/3\pi R_N)^{0.5}$ [15]. The condition for full ballistic transport ($a \ll \ell$) is totally verified in ab -plane

contacts, where $a_{ab} \approx 6 - 18$ nm. In c -axis junctions, where $a_c \approx 14 - 24$ nm but the conductance curves do not show any sign of heating [13], the presence of at least 30 parallel contacts in the junction area is expected.

After normalization, the conductance curves were fitted to the modified 3D Blonder-Tinkham-Klapwijk (BTK) model [18, 19, 20]. In the single-band form it contains three fitting parameters: The gap Δ , the barrier-height parameter Z and the broadening Γ which accounts for both intrinsic (quasiparticle lifetime) and extrinsic phenomena that broaden the AR conductance [19].

In order to increase the experimental resolution of our measurements we decided to perform part of the PCAR experiments at very low temperature in a Quantum Design measurement system (PPMS) with ^3He insert.

Fig. 2 (a) shows the normalized conductance curves (circles) of a typical ab -plane contact at various temperatures from 400 mK up to T_c . At any temperature the single-band 3D BTK model fits the data very well (solid lines). At the lowest T , the values of the fitting parameters are: $\Delta = 1.44$ meV, $\Gamma = 0.61$ meV and $Z = 0.75$. In panel (c) we display the order parameter Δ obtained from the data given in (a). Its temperature dependence almost perfectly follows the BCS-like expression (solid line) with $2\Delta(0)/k_B T_c = 2.98$ which is sensibly smaller than expected from BCS theory.

In Fig. 2 (b) and (d) we report the same data for a c -axis contact. As for the ab -plane case, the curves are well fitted by the single-band 3D BTK model which gives at 400 mK: $\Delta = 1.7$ meV, $\Gamma = 0.84$ meV and $Z = 0.97$. The temperature dependence of Δ is very close to the expected BCS one with a ratio $2\Delta(0)/k_B T_c = 3.48$, in best agreement with the weak-coupling BCS value.

It is worth noticing that the Z values observed in c -axis contacts (between 0.74 and 1.01) are systematically greater than those of ab -plane contacts (between 0.48 and 0.75). According to the 3D BTK model [20], this difference can be explained by the different Fermi velocities of CaC_6 in the ab plane ($v_{ab} = 0.54 \times 10^6$ m/s) and along c axis ($v_c = 0.29 \times 10^6$ m/s), thus confirming the directionality of our point contacts.

The AR curves shown in Fig. 1 and 2 are rather small in amplitude, as already observed in all the ‘soft’ PCAR measurements on MgB_2 and related compounds [11, 12, 13], resulting in Γ values substantially greater than those expected for the quasiparticle lifetime. As recently observed in lithographically fabricated Cu-Pt-Pb nanocontacts [21], this additional broadening can be explained by the presence of pair-breaking effects induced by the scattering in a thin disordered layer present at the NS interface. This is the case of our point contacts, due to a disordered layer on the surface of Ag grains that also makes the residual resistivity of the paint be five orders of magnitude greater than in pure Ag.

The reproducibility of the PCAR data was very good. Most of the contacts, obtained both in ^4He and in ^3He

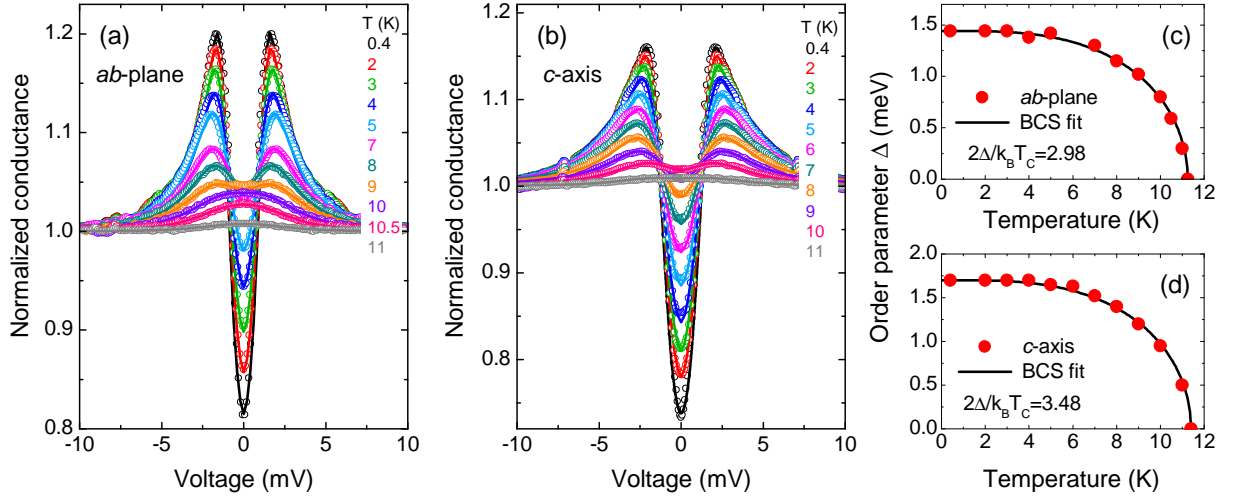


FIG. 2: (Color online) Normalized dI/dV vs. V curves at different temperatures down to 400 mK in an ab -plane contact (a) and in a c -axis one (b) (open circles). Solid lines: best-fit curves given by the single-band 3D BTK model. Panels (c) and (d) show the temperature dependency of the order parameter Δ (full circles) in the ab -plane direction and in the c -axis one, respectively, as determined from the BTK fits shown in (a) and (b). Solid lines are the BCS-like fits.

cryostat, show dI/dV curves and temperature dependencies of quality similar to that presented in Fig. 2. In 15 ab -plane contacts the order parameter $\Delta(0)$ ranged between 1.1 meV and 1.7 meV with the distribution shown in Fig. 3 (a). In 14 c -axis contacts $\Delta(0)$ ranged between 1.3 meV and 1.94 meV with the distribution shown in Fig. 3 (b). The figure also shows the Gaussian curves that best fit the distributions. They are peaked at $\Delta_{ab}(0)=1.35$ meV and $\Delta_c(0)=1.71$ meV and show standard deviations $s_{ab}=0.14$ meV and $s_c=0.08$ meV, respectively. The results in c -axis direction are in very good agreement with the gap values previously reported in Ref. 6, 7. A minority of contacts (3 in ab -plane and 3 in c -axis direction) have shown gap values between 2.1 and 2.4 meV, similarly to the results of Ref. 9.

The complex microscopical nature of our point contacts leaves some uncertainty about the true direction of current injection, particularly in the case of contacts on the side faces of the sample (i.e. ab -plane contacts) where, due to the intrinsic inhomogeneity of the cleaved surface, current injection along c axis is also possible.

However, the clear difference observed between the most probable $\Delta(0)$ values in ab -plane and c -axis contacts provides strong evidence for a gap anisotropy in CaC_6 .

In order to compare our results with the theoretical predictions of gap anisotropy in CaC_6 [10] we calculated the Andreev-reflection conductance curves by first-principles methods. We have a SN junction where $S = \text{CaC}_6$ and $N = \text{Ag}$. Let's label with the suffix $i = 1, 2, 3$ the three sheets of the CaC_6 Fermi surface (FS) (π and interlayer (IL) bands). If \mathbf{n} is the unitary vector in the direction of the injected current, $v_{i\mathbf{k},\mathbf{n}} = \mathbf{v}_{i\mathbf{k}} \cdot \mathbf{n}$ are the corresponding components of the Fermi velocities in the superconductor at wave vector \mathbf{k} for band i -th. Taking into account that Ag has a quasi-spherical FS and an almost constant Fermi velocity $v_N \neq v_{i\mathbf{k}}$, the corresponding quantity in the normal metal will be $v_{N,\mathbf{n}} = v_N$. Following Refs. 22, 23 we finally obtain the total AR conductance as:

$$\sigma(E, n) = \frac{\sum_i \langle \sigma_{i\mathbf{k}\mathbf{n}}(E) \frac{v_{i\mathbf{k},\mathbf{n}}^2}{v_{i\mathbf{k}}[v_{i\mathbf{k},\mathbf{n}} + v_N]^2} \rangle_{\text{FS}_i}}{\sum_i \langle \frac{v_{i\mathbf{k},\mathbf{n}}^2}{v_{i\mathbf{k}}[v_{i\mathbf{k},\mathbf{n}} + v_N]^2} \rangle_{\text{FS}_i}} \quad (1)$$

where: $\langle \rangle_{\text{FS}_i}$ is the integral over the i -th FS, i.e.

$$\langle \frac{v_{i\mathbf{k},\mathbf{n}}^2}{v_{i\mathbf{k}}[v_{i\mathbf{k},\mathbf{n}} + v_N]^2} \rangle_{\text{FS}_i} = \int_{v_{i\mathbf{k},\mathbf{n}} > 0} \frac{v_{i\mathbf{k},\mathbf{n}}^2}{[v_{i\mathbf{k},\mathbf{n}} + v_N]^2} \delta(E_{i\mathbf{k}}) d^3k.$$

$\sigma_{i\mathbf{k}\mathbf{n}}(E)$ is the BTK conductance of the i -th band expressed in terms of the quantities $N_{i\mathbf{k}}^q(E) = E/\sqrt{E^2 - \Delta_{i\mathbf{k}}^2}$ and $N_{i\mathbf{k}}^p(E) = \Delta_{i\mathbf{k}}/\sqrt{E^2 - \Delta_{i\mathbf{k}}^2}$ (whose real parts are the quasiparticle and the pair density of states in the same band, respectively) and of Z_n values. $\Delta_{i\mathbf{k}}$ is the gap value for band i -th at point \mathbf{k} over the FS, recently calculated from first principles [10]. The values of Z_n used in the calculation are taken similar to those of the curves shown

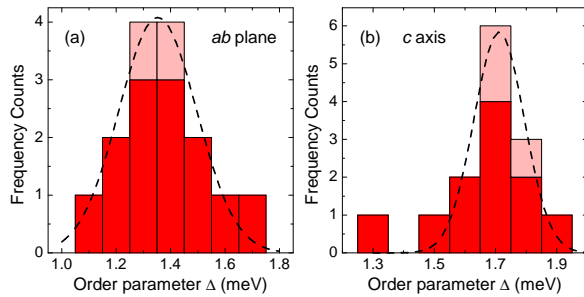


FIG. 3: (Color online) Distributions of the different $\Delta(0)$ values measured in ab -plane contacts (a) and in c -axis ones (b) at 4.2 K (red) and at 400 mK (light red). Dash black lines are the fits of the total distribution to a Gaussian curve.

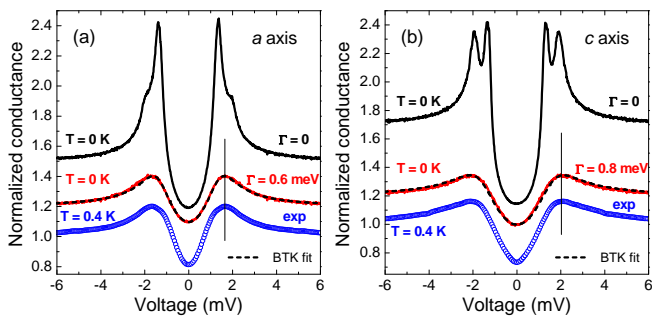


FIG. 4: (Color online) Theoretical AR conductances calculated at $T = 0$ by Eq. (1). (a) Current injected along the a axis with $Z = 0.75$ and $\Gamma = 0$ (black) and $\Gamma = 0.6$ (red); (b) current injected along the c axis with $Z = 1$ and $\Gamma = 0$ (black) and $\Gamma = 0.8$ (red). Experimental curves at 400 mK are shown for comparison (blue circles).

in Fig. 2, i.e. $Z_{ab} = 0.75$ and $Z_c = 1$. The explicit expression of $\sigma_{ikn}(E)$ can be found in Ref. 20.

The results of the calculations given by Eq. (1) are shown at $T = 0$ K and for a - and c -axis directions (top curves in Fig. 4 (a) and (b)). The conductance calculated along the b direction is almost identical to the one in a direction. At $T = 0$ the topology of the CaC_6 FS and the calculated anisotropy of the π and IL gaps result in a sizeable anisotropy of the AR conductance. In ab direction, it exhibits a sharp peak (related to the π gap) at about 1.38 meV and a broad shoulder (mainly related to the IL gap) at about 1.9 meV. In c direction, as expected from the shape of the FS, the role of the IL (Ca) gap becomes more important and the conductance shows two distinct peaks with almost the same height. However, for $\Gamma \neq 0$ even at $T = 0$ K these anisotropic features are rapidly smeared out. The middle curves of Fig. 4(a) and (b) show the effect on the theoretical conductances of a broadening similar to that observed at very low T in the experimental curves of Fig. 2. The conductances become similar to single-gap ones and can be perfectly fitted by single-gap 3D BTK curves, as shown in Fig. 4 (black dash lines). The use of more complex fitting models (anisotropic or two-band BTK) that we tested on our data does not improve the fit substantially, as already pointed out in Ref. 6, 9. In Fig. 4 the experimental ab -plane and c -axis conductances measured at 400 mK are included too (circles) in order to show the remarkable agreement with the theoretical curves for the same level of broadening. Although this broadening washes out the fine anisotropic structures of the conductance, a clear sign of the underlying gap anisotropy is still present since the 3D BTK fit of the theoretical conductances gives different order parameters in the two directions, $\Delta = 1.5$ meV ($\Gamma = 0.65$ meV, $Z = 0.765$) for a -axis direction and $\Delta = 1.7$ meV ($\Gamma = 0.92$ meV, $Z = 1.015$) for c -axis one. The c -axis value is in perfect agreement with the experimental results (both single curves at

400 mK and the peak of the distribution of the 14 different contacts). In the ab -plane case, the experimental Δ values from the curves at 400 mK and from the peak of the distribution of Fig. 3 (a) (ranging from 1.3 meV to 1.44 meV) are smaller than the value obtained from the fit of the theoretical conductance. This discrepancy could be ascribed to a possible slight overestimation of the small π gap (and, maybe, an underestimation of the large IL gap associated with Ca FS) in the theoretical calculations. This fact appears reasonable if one considers that the first-principle calculations of Ref. [10] led to an underestimation of T_c of about 17 %.

In conclusion, the first directional PCAR measurements in CaC_6 carried out also at $T = 400$ mK both along the ab -plane and the c -axis direction give strong and reproducible evidence of the predicted anisotropic nature of the superconducting gap in this GIC. New first-principles calculations of the expected anisotropy in the AR conductance curves fully support this conclusion and indicate that the actual gap anisotropy in CaC_6 could be even slightly greater than theoretically predicted.

We thank Lilia Boeri, O.V. Dolgov, E.K.U. Gross and I.I. Mazin for useful discussions. This work was done within the projects: PRIN (No. 2006021741) and Cybersar (cofunded by MUR under PON). V.A.S. acknowledges the support of RFBR (Proj. No. 06-02-16490).

-
- [1] T. E. Weller *et al.*, Nature Phys. **1**, 39 (2005).
 - [2] N. Emery *et al.*, Phys. Rev. Lett. **95**, 087003 (2005).
 - [3] J. S. Kim *et al.*, Phys. Rev. Lett. **99**, 027001 (2007).
 - [4] M. Calandra and F. Mauri, Phys. Rev. B **74**, 094507 (2006).
 - [5] I. I. Mazin *et al.*, Physica C **460-462**, 116 (2007).
 - [6] N. Bergeal *et al.*, Phys. Rev. Lett. **97**, 077003 (2006).
 - [7] G. Lamura *et al.*, Phys. Rev. Lett. **96**, 107008 (2006).
 - [8] J. S. Kim *et al.*, Phys. Rev. Lett. **96**, 217002 (2006).
 - [9] C. Kurter *et al.*, Phys. Rev. B **76**, 220502 (2007).
 - [10] A. Sanna *et al.*, Phys. Rev. B **75**, 020511(R) (2007).
 - [11] R.S. Gonnelli *et al.*, Phys. Rev. Lett. **89**, 247004 (2002).
 - [12] R.S. Gonnelli *et al.*, Phys. Rev. Lett. **97**, 037001 (2006).
 - [13] D. Daghero *et al.*, Phys. Rev. B **74**, 174519 (2006).
 - [14] Goutam Sheet, S. Mukhopadhyay, and P. Raychaudhuri, Phys. Rev. B **69**, 134507 (2004).
 - [15] Y.G. Naidyuk, I.K. Yanson, Point-Contact Spectroscopy, Springer Series in Solid-State Sciences, Vol. 145, 2004.
 - [16] J. S. Kim, unpublished results.
 - [17] A. Gauzzi *et al.*, Phys. Rev. Lett. **98**, 067002 (2007).
 - [18] G.E. Blonder, M. Tinkham and T.M. Klapwijk, Phys. Rev. B **25**, 4515 (1982).
 - [19] A. Plecenik *et al.*, Phys. Rev. B **49**, 10016 (1994).
 - [20] S. Kashiwaya *et al.*, Phys. Rev. B **53**, 2667 (1996).
 - [21] P. Chalsani *et al.*, Phys. Rev. B **75**, 094417 (2007).
 - [22] I.I. Mazin, Phys. Rev. Lett. **83**, 1427 (1999).
 - [23] A. Brinkman *et al.*, Phys. Rev. B **65**, 180517(R) (2002).